

Seasonal contrasts in the trends of landfalling tropical cyclone track density in China (1949–2023)

Article

Published Version

Creative Commons: Attribution-Noncommercial-No Derivative Works 4.0

Open Access

Wang, F., Zhao, J., Zhan, R., Yuan, C., Feng, X. ORCID: <https://orcid.org/0000-0003-4143-107X> and Tan, Y. (2025) Seasonal contrasts in the trends of landfalling tropical cyclone track density in China (1949–2023). *Geophysical Research Letters*, 52 (10). e2024GL114482. ISSN 1944-8007 doi: 10.1029/2024GL114482 Available at <https://centaur.reading.ac.uk/122730/>

It is advisable to refer to the publisher's version if you intend to cite from the work. See [Guidance on citing](#).

To link to this article DOI: <http://dx.doi.org/10.1029/2024GL114482>

Publisher: American Geophysical Union

All outputs in CentAUR are protected by Intellectual Property Rights law, including copyright law. Copyright and IPR is retained by the creators or other copyright holders. Terms and conditions for use of this material are defined in the [End User Agreement](#).

www.reading.ac.uk/centaur

CentAUR

Central Archive at the University of Reading

Reading's research outputs online

Geophysical Research Letters®



RESEARCH LETTER

10.1029/2024GL114482

Seasonal Contrasts in the Trends of Landfalling Tropical Cyclone Track Density in China (1949–2023)

Key Points:

- Landfalling tropical cyclone track density (LTD) shows a basin-wide decline, with an increase along the coastal East China (CEC)
- A clear seasonal contrast is observed in the CEC LTD trend, with an increase from August to October and a decline from May to July
- The LTD rise in late season is driven by northward diabatic heating, while the decline in early season by heating confined to the tropics

Supporting Information:

Supporting Information may be found in the online version of this article.

Correspondence to:

J. Zhao and R. Zhan,
jiuwei@nuist.edu.cn;
zhanrf@fudan.edu.cn

Citation:

Wang, F., Zhao, J., Zhan, R., Yuan, C., Feng, X., & Tan, Y. (2025). Seasonal contrasts in the trends of landfalling tropical cyclone track density in China (1949–2023). *Geophysical Research Letters*, 52, e2024GL114482. <https://doi.org/10.1029/2024GL114482>

Received 7 JAN 2025

Accepted 25 APR 2025

Author Contributions:

Conceptualization: Jiuwei Zhao,

Ruifen Zhan

Formal analysis: Fang Wang,

Jiuwei Zhao

Funding acquisition: Xiangbo Feng,

Yaheng Tan

Investigation: Fang Wang

Methodology: Jiuwei Zhao

Resources: Fang Wang, Jiuwei Zhao

Supervision: Jiuwei Zhao, Ruifen Zhan

Writing – original draft: Fang Wang,

Jiuwei Zhao, Ruifen Zhan

Writing – review & editing: Jiuwei Zhao,

Xiangbo Feng, Yaheng Tan

Fang Wang¹, Jiuwei Zhao¹ , Ruifen Zhan^{2,3} , Chaoxia Yuan¹ , Xiangbo Feng^{4,5} , and Yaheng Tan⁶

¹State Key Laboratory of Climate System Prediction and Risk Management/Institute of Climate and Application Research, Nanjing University of Information Science & Technology (NUIST), Nanjing, China, ²Department of Atmospheric and Oceanic Sciences & Institute of Atmospheric Sciences, Fudan University, Shanghai, China, ³CMA-FDU Joint Laboratory of Marine Meteorology, Shanghai, China, ⁴National Centre for Atmospheric Science and Department of Meteorology, University of Reading, Reading, UK, ⁵Department of Physics, Imperial College London, London, UK, ⁶Guizhou Climate Centre, Guiyang, China

Abstract The landfalling tropical cyclone track density (LTD) in China has shown an overall decreasing trend over the western North Pacific (WNP) while revealing an increase along the coastal East China (CEC) in the past several decades. This study further elucidates that the long-term LTD trend in the CEC exhibits a pronounced seasonal contrast that there is a significant increase from August to October, whereas a decline is observed from May to July. This seasonal reversal in the CEC LTD trend is attributed to the northward migration of an intensified diabatic heating source from May to October under global warming. This result is supported by a linear baroclinic model that incorporates realistic precipitation trends to parameterize diabatic heating over the WNP. Our finding underscores the critical role of local warming in modulating LTD trends, emphasizing its seasonal dependence rather than relying solely on sea surface temperature changes.

Plain Language Summary Tropical cyclones (TCs) can cause a significant natural hazard in China, and their landfall patterns in different seasons have changed over the past seven decades. This study investigates the seasonal trends in the landfalling TC track density (LTD) along the coastal East China (CEC) region from 1949 to 2023. The seasonal patterns in the CEC LTD reveal an interesting contrast that, from May to July (MJJ), the LTD in CEC has declined, but from August to October (ASO), there has been a noticeable increase. This seasonal reversal is linked to changes in atmospheric heating patterns due to global warming. During ASO, diabatic heating migrated northward, supporting more frequent TC landfalls along the CEC coast. In contrast, during MJJ, heating was more confined to the tropics, leading to fewer TCs making landfall. These findings highlight the seasonal dependence of TC landfall trends and suggest that local warming, rather than just sea surface temperatures, plays a significant role in shaping these patterns.

1. Introduction

Tropical cyclones (TCs) pose great threats to coastal regions. Upon landfall, TCs bring strong winds, heavy rainfall, and storm surges (Feng & Tsimplis, 2014; Shi et al., 2024), which often result in severe natural disasters that endanger lives and property (Emanuel, 2005; L. Liu et al., 2020; Park et al., 2014; Pielke et al., 2008; Zhang et al., 2009). Under global warming, both TC intensity and trajectory are shifting (Walsh et al., 2016; Zhao, Zhan, & Wang, 2018; Zhao et al., 2020), presenting new challenges for future climate predictions and disaster risk management. Therefore, expanding research on landfalling tropical cyclones (LTCs) is crucial for informing policymakers in the development of effective disaster prevention and mitigation policies.

Previous studies have shown that the intensity of LTCs in China has risen in recent decades (L. Liu & Wang, 2020; Mei & Xie, 2016; Zhao, Zhan, Wang, & Xu, 2018), leading to increased destructiveness, especially along coastal regions (R. C. Y. Li et al., 2017). This intensification can be partly attributed to the rise in sea surface temperatures (SST), which triggers a climate shift in the western North Pacific (WNP) and fosters the development of stronger LTCs affecting China (Gao et al., 2021). Some studies also have suggested a slowdown in TC translation speed over the WNP and revealed a slower decay of LTCs in a warming world (L. Li & Chakraborty, 2020). This significantly increases the annual average overland duration of a TC (Chen et al., 2011), and the frequency of extreme precipitation events induced by LTCs (Lai et al., 2024; K. S. Liu & Chan, 2020; L. Liu et al., 2022), particularly in southeastern coastal China (L. Liu & Wang, 2020). Additionally, the tracks and

© 2025. The Author(s).

This is an open access article under the terms of the [Creative Commons Attribution-NonCommercial-NoDerivs License](https://creativecommons.org/licenses/by/4.0/), which permits use and distribution in any medium, provided the original work is properly cited, the use is non-commercial and no modifications or adaptations are made.

distribution patterns of LTCs have exhibited shifts, with landfall locations moving further north (Feng, 2024; Feng et al., 2021), more TCs affecting East China coastal areas and less cases moving into the South China Sea (SCS; Huangfu et al., 2023; Kossin et al., 2014; Tang et al., 2024; Tu et al., 2009; Wu et al., 2005). These shifts are closely linked to changes in the large-scale steering flow, which is associated with the westward expansion and strengthening of the WNP subtropical high (Wu et al., 2005; Zhou et al., 2018).

Despite these advancements, current studies still face limitations. Especially, most previous studies have focused on interannual or longer-term changes (Chan & Xu, 2009; R. C. Y. Li et al., 2017; Mei & Xie, 2016; Zhang et al., 2013), often overlooking the impacts of seasonal variability (Shan et al., 2023; Song et al., 2021) and its complex environmental factors in shaping LTC patterns. Under global warming, the seasonal variations of LTCs and their underlying driving factors remain uncertain. This study aims to uncover the seasonal trends of LTCs in China and their underlying mechanisms driving these changes under global warming. By enhancing our understanding of the climatic dynamics behind TC activity, this research provides valuable insights into the observed long-term trend in landfall TC activities, contributing to improved knowledge for disaster prevention and mitigation strategies in coastal regions.

2. Data and Methods

2.1. TC and Reanalysis Data Sets

This study uses TC records from 1949 to 2023, obtained from the Shanghai Typhoon Institute of China Meteorological Administration (CMA; Lu et al., 2021; Ying et al., 2014). These records are relatively reliable, as they are derived from a network of meteorological observatories situated along the coastal regions of China. Over the past 75 years, the CMA has documented 667 LTCs, with the majority occurring during June–September, accounting for about 90% of the total LTCs. The LTC track density (LTD) is calculated using longitudinal and latitudinal information at 6-hr intervals. The number of LTD was calculated within 5° ranges centered on each grid point with a grid spacing of 1°. This approach can reduce uncertainty and bias in determining of LTD locations and also suppressing the noise in statistical analysis. The monthly precipitation and three-dimensional wind data are derived from the fifth-generation European Centre for Medium-Range Weather Forecasts (ECMWF) reanalysis (ERA5) for the same period (Hersbach et al., 2020).

2.2. Decomposition of LTD

Following previous studies (Yokoi et al., 2013; Zhao et al., 2020), we decomposed the changes of TC tracks into three components: the location shift of TC genesis, the length change of TC tracks, and nonlinear interactions between genesis and tracks. The LTD in a 5° grid box can be written as follows:

$$\overline{T(A)} = \iint_c \overline{g(A_0)} \cdot \overline{t(A, A_0)} dA_0 \quad (1)$$

here, $\overline{T(A)}$ is the LTD in grid box A, $g(A_0)$ is the LTC genesis frequency in grid box A_0 , and $t(A, A_0)$ stands for the probability for a LTC formed in grid box A_0 to travel into grid box A. The subscript c is the entire domain of the WNP over which the integration is performed. For the period 1949–2023, the LTD anomalies (Δ) relative to the climatological mean in grid box A are calculated as:

$$\Delta T(A) = \iint_c \Delta g(A_0) \cdot \overline{t(A, A_0)} dA_0 + \iint_c \Delta t(A_0) \cdot \overline{g(A, A_0)} dA_0 + \iint_c \Delta g(A_0) \cdot \Delta t(A, A_0) dA_0 \quad (2)$$

The first term quantifies the contribution of genesis location shift and frequency number change under global warming by assuming the TC tracks unchanged; the second term evaluates the track length or duration time contribution if the TC genesis information remains constant under warming and the third term indicates a nonlinear contribution from changes of both genesis location (or frequency) and track length (or duration time).

2.3. Linear Baroclinic Model (LBM) Experiment

To investigate the mechanism responsible for the season contrast of LTD trend, we employed a Linear Baroclinic Model (LBM; Watanabe & Jin, 2003) to validate physical processes derived from observations and reanalysis. In this study, we did not use the default idealized SST forcing structure based on an elliptical circle (Watanabe &

Jin, 2003). Instead, we parameterized the realistic precipitation (P , mm day^{-1}) to the diabatic heating (H , K day^{-1}) based on their linear relationship:

$$H = \frac{P \times \rho \times L_v}{C_p \times (p/g)} \times 10^{-3} [\text{K day}^{-1}] \quad (3)$$

where all other variables are constant except H and P that ρ represents water density, L_v is the latent heat constant, C_p stands for specific heat at constant pressure, p denotes mean surface pressure, and g is gravitational acceleration. Seasonal mean atmospheric fields from 1949 to 2023 are adopted as initial conditions for each experiment, encompassing zonal wind, meridional wind, temperature, specific humidity, and surface pressure. Three sets of sensitive experiments were conducted in this study. Each experiment is integrated for 200 days and we only used results when the LBM reaches the quasi-steady state, which is around day 30.

Three sensitivity experiments are designed with the following forcing configurations: The June-July (JJ) run was forced by the precipitation anomalies, derived from the linear trend of JJ averaged precipitation from 1949 to 2023. The initial conditions were based on the JJ averages. The August-September (AS) run used the precipitation trend increments for August and September averaged from 1949 to 2023. We also tested an August-October run forced by the contemporary precipitation trend and found that the results were consistent with those of the AS run. An additional experiment, the AS-JJ run, was designed to capture the precipitation difference between the AS and JJ trends, providing insights into the seasonal variations of LTD in China.

2.4. Landfalling TC Track Clustering Algorithm

The clustering algorithm employed in this study is the widely-used K -means clustering method (Camargo et al., 2007; Gaffney et al., 2004, 2007; Jain, 2010). This unsupervised machine learning algorithm is capable of learning features from data without external guidance. For this analysis, we used the Curve Cluster Toolbox to extract the mean TC tracks and genesis locations across different periods, with the parameter $K = 1$.

3. Results

Over the past 75 years (1949–2023), a total 667 TCs have made landfall across mainland China and Taiwan, as documented by the CMA data (Figure 1a). Some dissipated after landfall, while others turned after making landfall. Consistent with previous studies (Chen et al., 2011), the time series of LTC annual frequency displays an insignificant decreasing trend over this period, followed by notable decadal fluctuations (Figure 1b). It is worth mentioning that, in this study, we excluded tropical depressions to reduce the data uncertainty, although our additional analysis showed that the results are relatively consistent with and without their inclusion. Despite the lack of significance in the overall LTC trend, a significant decreasing trend in LTD has been identified over both the deep tropics and higher latitudes (Figure 1c). Notably, in contrast to the general decline in LTC frequency, an increasing trend in LTD is evident along the coastal East China (CEC) region, although only some areas passed by the 90% confidence level (Figure 1c). It suggests that the spatial distribution of LTD trends exhibits distinct regional characteristics.

To further investigate, we examined the seasonal distributions of LTC frequency with different intensity categories (Figure 1d). Most landfalls occur during May–October, with minimal activity during other months. Among them, the typhoon intensity category occurs most frequently, followed by severe tropical storm intensity, with the least occurring at the super typhoon intensity category. The former peaks in July and August, while the latter reaches the maximum in September. This distinct seasonality prompted an in-depth analysis of monthly LTD trends (Figure S1 in Supporting Information S1). In May, the LTD exhibits a nearly basin-wide decreasing trend, with the SCS LTD showing statistically significant reductions (Figure S1a in Supporting Information S1). From June to July (JJ), a slightly increasing trend of LTD is observed near the Philippines, and the northern SCS shifted to a significant increase, while a decreasing trend is apparent over the CEC and east of Taiwan, as marked by a red box (Figures S1b and S1c in Supporting Information S1). Intriguingly, during August–October (ASO), the LTD trends are reversed: significant decreases are seen from the SCS to the east of the Philippines during August–September, while increases are witnessed over the CEC, especially significant in August and October (Figures S1d–S1f in Supporting Information S1).

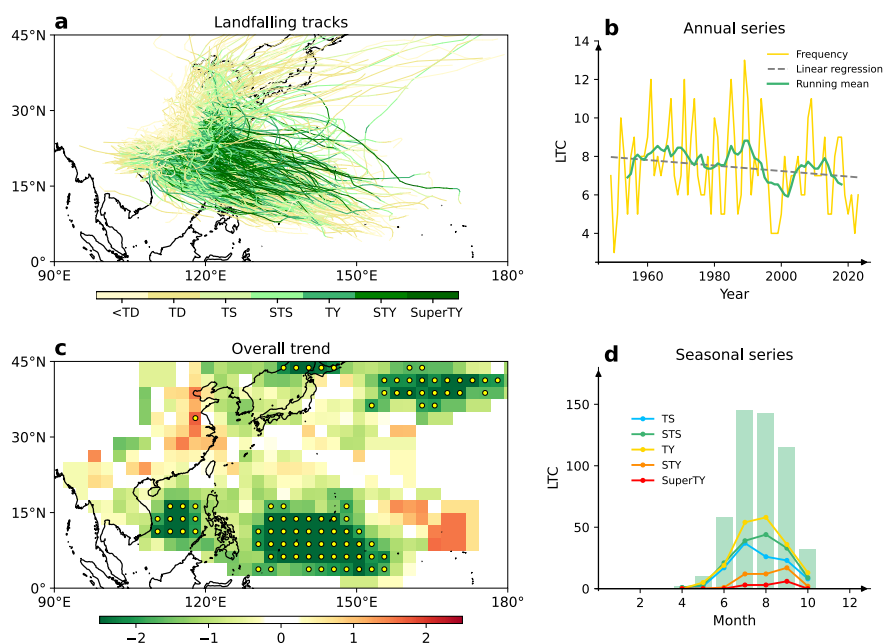


Figure 1. Statistics of landfalling tropical cyclones (LTCs). (a) LTC tracks during 1949–2023; (b) the time series of annual LTC frequency (yellow line) with the linear trend (dashed gray line) and 11-year running mean (green line); (c) the linear trend of annually averaged track density from 1949 to 2023; and (d) seasonal distribution of LTC with different Tropical cyclone intensity categories. The yellow dots in (c) represent regions at 90% confidence level using the student's *t*-test.

This seasonal contrast is represented by the LTD trends based on the MJJ and ASO seasons (Figures 2a and 2e). To explore the possible mechanisms of this seasonal contrast marked in the red box, we decomposed the LTD change in MJJ and ASO into contributions from genesis frequency, track, and a nonlinear term, following the decomposition method introduced earlier (Figures 2b–2d and 2f–2h). The slight increase in LTD over the Philippines in MJJ (Figure 2a) is mainly contributed by an increasing trend in TC genesis term while keeping the TC track length unchanged under global warming (TCGF; Figure 2b). The track term isolates the effects of track length or duration change when keeping TC genesis (numbers and location) unchanged (Figure 2c). The nonlinear term captures the combined effect of changes in both genesis and track under global warming. However, the increase of LTD in SCS in JJ due to the genesis term (Figure 2b) is offset by the decrease in both track term (Figure 2c) and nonlinear term (Figure 2d), leading to an insignificant increase of LTD (Figure 2a). Conversely, the decreasing LTD trend over the CEC region in MJJ is primarily attributed to reductions in TC track term and nonlinear term (Figures 2c and 2d). In ASO, the increasing LTD trend over the CEC (Figure 2e) is dominantly attributed to changes in track probability and nonlinear term (Figures 2g and 2h), with minimal contributions from genesis frequency (Figure 2f). Similarly, the decreasing LTD trend over the Philippines (Figure 2e) is closely associated with changes in nonlinear term (Figure 2h). When both factors—decreasing TC genesis and increasing TC track length—are considered together, their joint effect amplifies the LTD increase in the nonlinear term (Figure 2h), leading to the observed trend. It strongly indicates that the seasonal reversal of LTD trends over the CEC between MJJ and ASO is primarily driven by changes in track probability and the nonlinear processes.

Previous studies have attributed the increasing trend of LTD over the CEC to the local (Mei et al., 2015) or global (Zhao et al., 2020) SST warming. However, few studies have addressed the seasonal contrast in LTD trends between MJJ and ASO over the WNP and its underlying causes. A question arises as to whether this seasonal contrast is driven by local circulation changes or is connected to the remote forcings under global warming. To address this question, we divided the precipitation and low-level winds at 850 hPa into two periods: the prior period (1949–1985) and the post period (1986–2023), and compared their differences during the active TC months (JJ vs. AS). Note that we also tested different seasonal averages, such as August and October (AO), and August to October (ASO; Figure S2 in Supporting Information S1), with consistent results. Considering the seasonal evolution of the mean state, we select JJ and AS seasons to avoid potential discontinuity in the mean state.

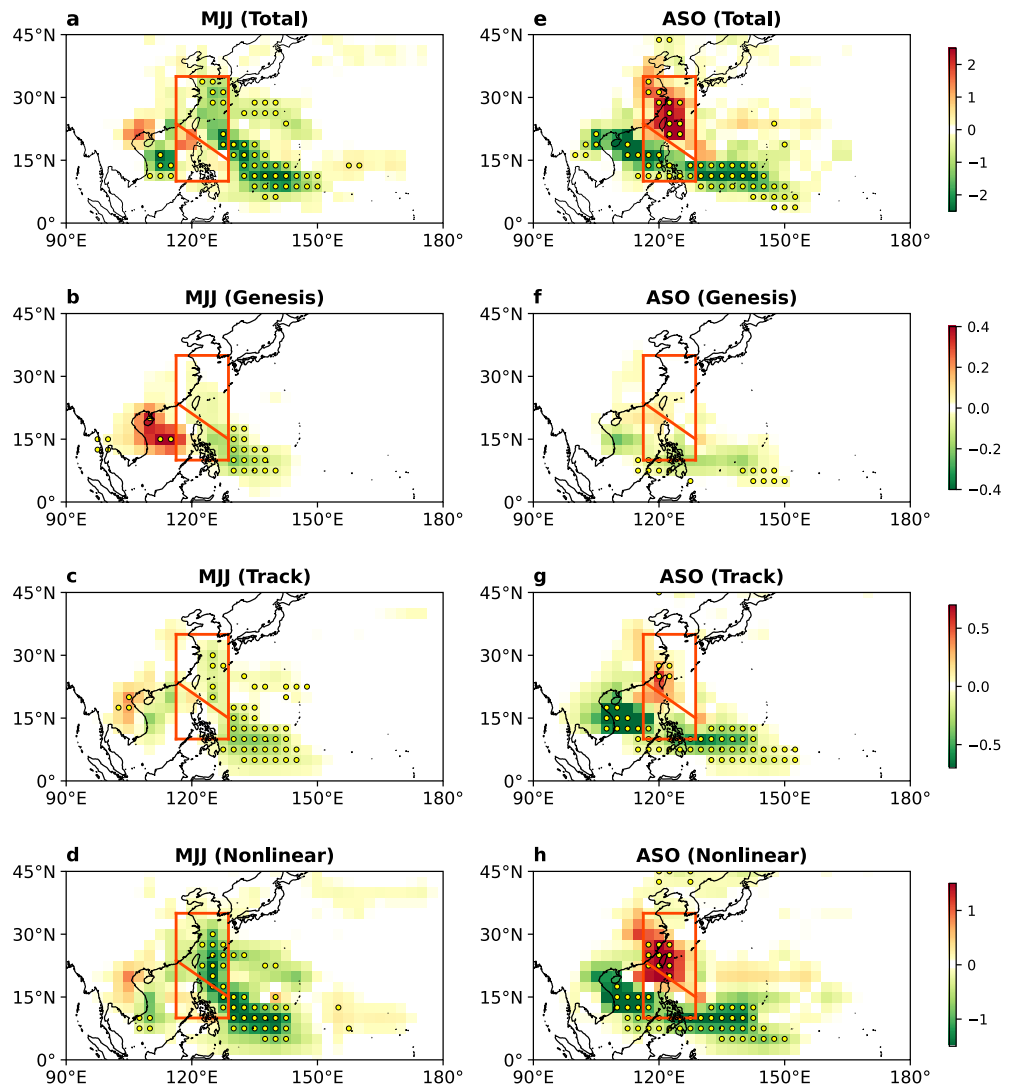


Figure 2. Composite differences of track density for May-July (MJJ; left) and August-October (ASO; right) and their decomposition between the post and prior periods. (a, e) Composite differences of (a) MJJ-summed and (e) ASO-summed LTDs; (b–h) the contributions from (b, f) tropical cyclone (TC) genesis, (c, g) TC track probability, and (d, h) the nonlinear process to the (left) MJJ and (right) ASO landfalling tropical cyclone track changes. The yellow dots represent regions at 90% confidence level using the student's *t*-test.

Figure S3 in Supporting Information S1 shows the mean states of vorticity and low-level winds (left two panels), as well as precipitation and steering flow (right two panels), in prior and post periods. During JJ, the monsoon trough remains weak and is confined to the west of 140°E in both periods (Figures S3a and S3b in Supporting Information S1), limiting TC genesis and tracks over the SCS and east of the Philippines (Figures S4a and S4b in Supporting Information S1). Their differences in 850-hPa winds and vorticity between post and prior periods during JJ (Figure 3a) show a clear anomalous cyclonic circulation south of 25°N and an anomalous anticyclonic circulation north of 25°N. It is tightly corresponded to positive precipitation anomalies (Figure 3b), contributing to a weak increase in LTD near the Philippines (Figure 2a). However, the anticyclonic circulation anomalies in Figure 3a could contribute to the decrease in LTC genesis term (Figure 2b) over the CEC. The eastward steering flow anomalies over the CEC (Figure 3b) result in the decrease in LTD in Figure 2c. The jointly low-level circulation and steering flow change (Figures 3a and 3b) could induce the decrease in LTD over the CEC in JJ reflected by the nonlinear term (Figure 2d). During AS, the monsoon trough intensifies, extending eastward and shifting northward in response to radiative forcing in both periods (Figures S3e and S3f in Supporting Information S1), leading to the seasonal northward shift of LTD (Figures S4d–S4f in Supporting Information S1).

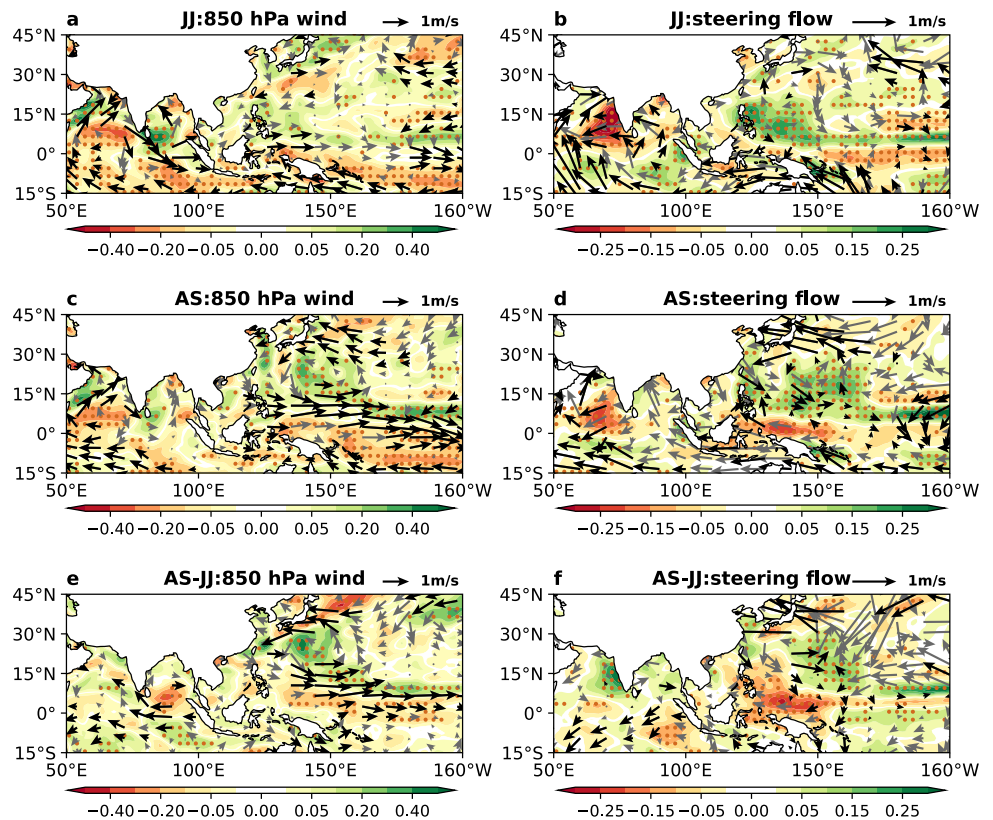


Figure 3. Seasonal differences of 850-hPa winds (m s^{-1}), vorticity (10^{-5} s^{-1}), steering flow (m s^{-1}) and precipitation (mm d^{-1}) between post and prior periods. (a) June–July (JJ) difference of vorticity (shaded) and 850-hPa winds (vector) between for post (1986–2023) and prior (1949–1985) periods; (b) same as (a) but for JJ precipitation (shaded) and steering flow (vector) averaged from 850 to 200 hPa; (c) August–September (AS) difference of vorticity (shaded) and 850-hPa winds (vector) between for post (1986–2023) and prior (1949–1985) periods; (d) same as (c) but for the AS precipitation and steering flow; (e) the difference between AS (c) and JJ (a) seasons; and (f) the difference between (d) and (b). Scatter points and black vectors indicate areas above 90% confidence level based on Student's *t*-test.

Comparing AS with JJ, cyclonic circulation anomalies (Figure 3c) and positive precipitation anomalies (Figure 3d) shift northeastward. The westerly steering flow anomalies over the tropics (Figure 3d) leads to the decrease in LTD east of Philippines meanwhile the easterly steering flow anomalies lead to the increase in LTD toward the CEC (Figure 2e). Lastly, easterly wind anomalies over the Indian Ocean and westerly wind anomalies over the equatorial Pacific induce the downward motion near the SCS (Figure 3f), potentially suppressing LTD in this region (Figures 2e–2h and Figure S4f in Supporting Information S1).

Compared the prior and post periods, we observe an intensified precipitation anomaly between AS and JJ in the post period (Figures S3k vs. S3l in Supporting Information S1). The intensified regional precipitation results in stronger cyclonic circulation anomalies over the CEC during the post period compared to the prior period (Figure 3f). Another prominent feature is that the precipitation anomaly over the WNP shows a poleward migration as time, with the center of positive diabatic heating located east of Taiwan, while negative precipitation anomalies dominated over the SCS and east of Philippines (Figure 3f). Consequently, the LTD significantly increases over the CEC and decreases over the Philippines in AS, while the opposite trend is observed in JJ (Figures 2a and 2e).

The contrast differences between LTD over the Philippines and CEC are predominantly influenced by the seasonal movement of the mean state. From JJ to AS, the mean-state warm SST moves northward, leading to the northward migration of cyclonic circulation anomalies between 10°N and 30°N during both the prior and post periods (Figures S3i and S3j in Supporting Information S1). In JJ, cyclonic circulation anomalies over the SCS

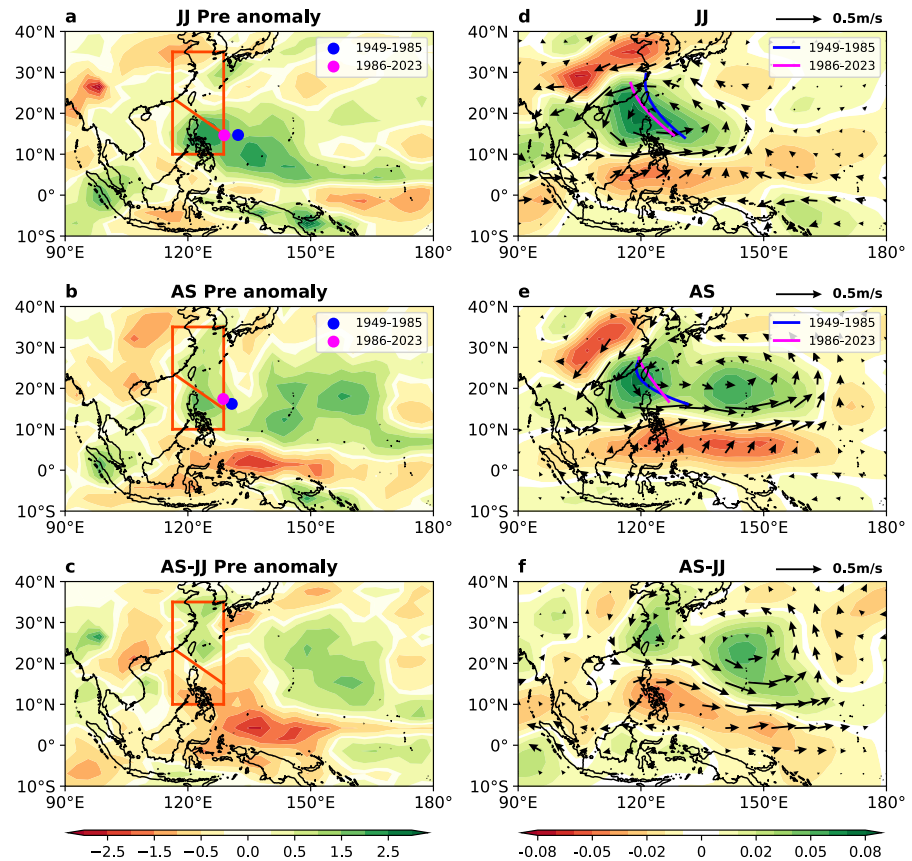


Figure 4. Diabatic heating sources and circulation responses in the Linear Baroclinic Model. (a, b) precipitation anomalies during (a) June–July (JJ) and (b) August–September (AS) between the post and prior periods, parameterized as a heating source in the LBM; (c) difference in precipitation anomalies between AS and JJ; (d, e) 850-hPa vorticity responses to the (d) JJ and (e) AS precipitation anomalies; (f) difference in 850-hPa vorticity responses between AS and JJ. The blue (magenta) dots represent the average genesis points of landfalling tropical cyclones (LTCs) for the prior (post) periods, while the blue (magenta) lines indicate the average tracks of LTCs for the prior (post) periods.

lead to a slight local increase in LTD (Figure 2a), while anticyclonic circulation anomalies (Figure 3e) and westerly steering flow anomalies (Figure S4c in Supporting Information S1) over the CEC result in a local decrease in LTD. As the low-level cyclonic circulation migrates northward (Figure 3f), it enhances LTD over the CEC in AS (Figure 2e; Figures S3g–S3i in Supporting Information S1) while suppressing LTD in deep tropics due to westward steering flow (Figure 3f).

We further verified our results through LBM experiments. The JJ precipitation anomaly between the post and prior periods over the WNP (90°E–180°; 10°S–40°N) was parameterized as the heating source in the model (JJ Run), with the initial condition based on the JJ climatological circulations, including sea level pressure, multi-level winds, temperature, and humidity on T42 spectral grids (Figure 4a). The JJ Run shows a significant cyclonic circulation accompanied by upward motion over the SCS and east of Philippines, while easterly wind anomalies dominate the tropics east of 150°E. This anomalous circulation closely assembles the reanalysis differences in JJ between the post and prior period (Figure 3a), leading to a decreasing trend of LTD east of the Philippines and over the CEC, but a slightly increasing trend over the Philippines (Figures 2a and 2b). The AS Run, forced by the heating source parameterized from the climatological AS precipitation anomaly between the post and prior periods (Figure 4b), revealing a significantly northward-shifted positive precipitation anomaly compared to the JJ season. This shows a strong cyclonic circulation anomaly with the center east of Taiwan (Figure 4e). However, the tropics south of 10°N are dominated by downward motion. As a result, LTD decreases significantly in the tropics but increases over the CEC (Figure 2e and Figure S4f in Supporting Information S1).

Lastly, the AS-JJ precipitation difference between the post and prior periods was used as the forcing in a separate experiment (Figure 4c). The resulting dipole precipitation anomalies (Figure 4c) induce cyclonic circulation anomalies east of Taiwan and downward motion over the SCS and east of the Philippines (Figure 4f). This configuration is favorable for more LTD over the CEC in AS while suppressing LTD over the Philippines, reversing the trends observed in JJ.

Figure 4 also compares the JJ and AS seasons between the prior and post periods using a clustering analysis algorithm. In the post period, the average track in JJ shifts southward compared to the prior period (Figure 4d), while the average track in AS moves northward (Figure 4e). These results further corroborate the phenomenon of seasonal reversal in LTD.

4. Summary and Discussion

In this study, we explored the long-term trends in landfalling TC in China from 1949 to 2023, uncovering notable spatial and seasonal variations. While the overall trend shows a nearly basin-wide decrease in LTD over the WNP, an exception is observed over the coastal region of East China (CEC), where a localized increasing trend is evident. This finding aligns with previous studies (R. C. Y. Li et al., 2017), but we extended the analysis to reveal a striking seasonal dependence. Specifically, during May-July (MJJ), the LTD trend decreases significantly over the CEC while showing a slight increase near the Philippines. From August to October (ASO), the trend undergoes a reversal, increasing over the CEC and decreasing from the SCS to the east of the Philippines.

This seasonally dependent reversal in LTD trends is primarily attributed to the northward migration of intensified precipitation anomalies driven by global warming. In MJJ, equatorial positive precipitation anomalies generate an anomalous cyclonic circulation over the Philippines, promoting local TC (TC) genesis and tracks. However, the easterly wind anomalies on the northern and eastern flanks of this cyclonic circulation suppress LTD over the CEC. As the climate warms and precipitation anomalies shift northward in ASO, the associated cyclonic circulation anomalies follow suit. This shift favors increased LTD over the CEC, while LTD near the Philippines is reduced due to anomalous downward motion during ASO (Figures 4d and 4e).

We focused on the effects of local WNP warming. However, we acknowledge that remote forcing linked to SST warming patterns could also contribute to a northward shift in precipitation. We also tested the WNP circulation response to diabatic forcing over the Indian Ocean and the entire tropics excluding the WNP using the LBM (Figure S5 in Supporting Information S1). We find that neither experiment can reproduce the realistic cyclonic circulation anomalies over the WNP, which indicates that the local WNP forcing plays a dominant role. In addition, we observed distinct spatial constraints on circulation anomalies. In MJJ and ASO, cyclonic circulation anomalies are confined to the western WNP, while the eastern WNP remains dominated by easterly wind anomalies. By October and November, the easterly wind anomalies extend across the entire WNP (Figure S6 in Supporting Information S1), consistent with previous studies (Zhao et al., 2020). Last, we observed that the LTC frequency (Figure 1b) also shows decadal fluctuation, which may also reflect the decadal variability in TC tracks over the WNP. Previous studies have suggested that decadal climate variability, such as the Pacific Decadal Oscillation (PDO; Chan, 2007; Wang et al., 2010) and the Interdecadal Pacific Oscillation (IPO; K. S. Liu & Chan, 2008; Zhao et al., 2020), can modulate the genesis location and track density, thereby influencing their landfall probability in East Asia.

Data Availability Statement

The LBM model data used in this study can be downloaded from https://ccsr.aori.u-tokyo.ac.jp/~lbm/sub/lbm_1.html. The IBTrACS data (Gahtan et al., 2024) is downloaded from <https://doi.org/10.25921/82ty-9e16>. The monthly precipitation and three-dimensional wind data are derived from the ERA5 reanalysis data set (Hersbach et al., 2023), which can be downloaded from <https://cds.climate.copernicus.eu/>. The Clustering Toolbox can be accessed at <http://www.datalab.uci.edu/resources/CCT/>. Calculations and Figures were made with Python v3.9.12 (Van Rossum & Drake, 2009) available at <https://www.anaconda.com>.

Acknowledgments

This study is supported jointly by the National Natural Science Foundation of China (Grants 42088101 and 42305051), the Shanghai Science and Technology Committee Project (Grant 23DZ1204703), and the National Natural Science Foundation of China (Grant 42105022).

References

Camargo, S. J., Robertson, A. W., Gaffney, S. J., Smyth, P., & Ghil, M. (2007). Cluster analysis of typhoon tracks. Part I: General properties. *Journal of Climate*, 20(14), 3635–3653. <https://doi.org/10.1175/JCLI4188.1>

Chan, J. C. L. (2007). Decadal variations of intense typhoon occurrence in the western North Pacific. *Proceedings of the Royal Society A: Mathematical, Physical and Engineering Sciences*, 464(2089), 249–272. <https://doi.org/10.1098/rspa.2007.0183>

Chan, J. C. L., & Xu, M. (2009). Inter-annual and inter-decadal variations of landfalling tropical cyclones in East Asia. Part I: Time series analysis. *International Journal of Climatology*, 29(9), 1285–1293. <https://doi.org/10.1002/joc.1782>

Chen, X., Wu, L., & Zhang, J. (2011). Increasing duration of tropical cyclone over China. *Geophysical Research Letters*, 38(2), L02708. <https://doi.org/10.1029/2010GL046137>

Emanuel, K. (2005). Increasing destructiveness of tropical cyclones over the past 30 years. *Nature*, 436(7051), 686–688. <https://doi.org/10.1038/nature03906>

Feng, X. (2024). Translation speed slowdown and poleward migration of western North Pacific tropical cyclones. *npj Climate and Atmospheric Science*, 7(1), 1–11. <https://doi.org/10.1038/s41612-024-00748-5>

Feng, X., Klingaman, N. P., & Hodges, K. I. (2021). Poleward migration of western North Pacific tropical cyclones related to changes in cyclone seasonality. *Nature Communications*, 12(1), 6210. <https://doi.org/10.1038/s41467-021-26369-7>

Feng, X., & Tsimplis, M. N. (2014). Sea level extremes at the coasts of China. *Journal of Geophysical Research: Oceans*, 119(3), 1593–1608. <https://doi.org/10.1002/2013JC009607>

Gaffney, S. (2004). *Probabilistic curve-aligned clustering and prediction with regression mixture models [dissertation]*. University of California.

Gaffney, S. J., Robertson, A. W., Smyth, P., Camargo, S. J., & Ghil, M. (2007). Probabilistic clustering of extratropical cyclones using regression mixture models. *Climate Dynamics*, 29(4), 423–440. <https://doi.org/10.1007/s00382-007-0235-z>

Gahtan, J., Knapp, K. R., Schreck, C. J., III, Diamond, H. J., Kossin, J. P., & Kruk, M. C. (2024). International best track archive for climate stewardship (IBTrACS) Project, version 4.01 [Dataset]. *NOAA National Centers for Environmental Information*. <https://doi.org/10.25917/82ty-9e16>

Gao, S., Chen, Z., Zhang, W., & Shen, X. (2021). Effects of tropical North Atlantic sea surface temperature on intense tropical cyclones land-falling in China. *International Journal of Climatology*, 41(2), 1056–1065. <https://doi.org/10.1002/joc.6732>

Hersbach, H., Bell, B., Berrisford, P., Biavati, G., Horányi, A., Muñoz Sabater, J., et al. (2023). ERA5 hourly data on single levels from 1940 to present [Dataset]. *Copernicus Climate Change Service (C3S) Climate Data Store (CDS)*. <https://doi.org/10.24381/cds.bd0915c6>

Hersbach, H., Bell, B., Berrisford, P., Hirahara, S., Horányi, A., Muñoz-Sabater, J., et al. (2020). The ERA5 global reanalysis [Dataset]. *Quarterly Journal of the Royal Meteorological Society*, 146(730), 1999–2049. <https://doi.org/10.1002/qj.3803>

Huangfu, J., Tang, Y., He, Z., Huang, G., Chen, W., & Huang, R. (2023). Influence of synoptic-scale waves on the interdecadal change in tropical cyclone activity over the western North Pacific in the early 2010s. *Geophysical Research Letters*, 50(5), e2022GL102095. <https://doi.org/10.1029/2022GL102095>

Jain, A. K. (2010). Data clustering: 50 years beyond K-means. *Pattern Recognition Letters*, 31(8), 651–666. <https://doi.org/10.1016/j.patrec.2009.09.011>

Kossin, J. P., Emanuel, K. A., & Vecchi, G. A. (2014). The poleward migration of the location of tropical cyclone maximum intensity. *Nature*, 509(7500), 349–352. <https://doi.org/10.1038/nature13278>

Lai, Y., Gu, X., Wei, L., Wang, L., Slater, L., Li, J., et al. (2024). Slower-decaying tropical cyclones produce heavier precipitation over China. *npj Climate and Atmospheric Science*, 7(1), 99. <https://doi.org/10.1038/s41612-024-00655-9>

Li, L., & Chakraborty, P. (2020). Slower decay of landfalling hurricane in a warming world. *Nature*, 587(7833), 230–234. <https://doi.org/10.1038/s41586-020-2867-7>

Li, R. C. Y., Zhou, W., Shun, C. M., & Lee, T. C. (2017). Change in destructiveness of landfalling tropical cyclones over China in recent decades. *Journal of Climate*, 30(9), 3367–3379. <https://doi.org/10.1175/JCLI-D-16-0258.1>

Liu, K. S., & Chan, J. C. L. (2008). Interdecadal variability of western North Pacific tropical cyclone tracks. *Journal of Climate*, 21(17), 4464–4476. <https://doi.org/10.1175/2008JCLI2207.1>

Liu, K. S., & Chan, J. C. L. (2020). Recent increase in extreme intensity of tropical cyclones making landfall in South China. *Climate Dynamics*, 55(5), 1059–1074. <https://doi.org/10.1007/s00382-020-05311-5>

Liu, L., & Wang, Y. (2020). Trends in landfalling tropical cyclone-induced precipitation over China. *Journal of Climate*, 33(6), 2223–2235. <https://doi.org/10.1175/JCLI-D-19-0693.1>

Liu, L., Wang, Y., Zhan, R., Xu, J., & Duan, Y. (2020). Increasing destructive potential of landfalling tropical cyclones over China. *Journal of Climate*, 33(9), 3731–3743. <https://doi.org/10.1175/JCLI-D-19-0451.1>

Liu, L., Yang, B., Jiang, X., Luo, Y., & Ren, F. (2022). Changes in tropical cyclone-induced extreme hourly precipitation over China during 1975–2018. *Journal of Climate*, 35(22), 7339–7352. <https://doi.org/10.1175/JCLI-D-21-0736.1>

Lu, X., Yu, H., Ying, M., Zhao, B., Zhang, S., Lin, L., et al. (2021). Western North Pacific tropical cyclone database created by the China meteorological administration [Dataset]. *Advances in Atmospheric Sciences*, 38(4), 690–699. <https://doi.org/10.1007/s00376-020-0211-7>

Mei, W., & Xie, S.-P. (2016). Intensification of landfalling typhoons over the northwest Pacific since the late 1970s. *Nature Geoscience*, 9(10), 753–757. <https://doi.org/10.1038/ngeo2792>

Mei, W., Xie, S.-P., Zhao, M., & Wang, Y. (2015). Forced and internal variability of tropical cyclone track density in the western North Pacific. *Journal of Climate*, 28(1), 143–167. <https://doi.org/10.1175/JCLI-D-14-00164.1>

Park, D.-S. R., Ho, C.-H., & Kim, J.-H. (2014). Growing threat of intense tropical cyclones to East Asia over the period 1977–2010. *Environmental Research Letters*, 9(1), 014008. <https://doi.org/10.1088/1748-9326/9/1/014008>

Pielke, R. A., Gratz, J., Landsea, C. W., Collins, D., Saunders, M. A., & Musulin, R. (2008). Normalized hurricane damage in the United States: 1900–2005. *Natural Hazards Review*, 9(1), 29–42. [https://doi.org/10.1061/\(ASCE\)1527-6988\(2008\)9:1\(29\)](https://doi.org/10.1061/(ASCE)1527-6988(2008)9:1(29))

Shan, K., Lin, Y., Chu, P.-S., Yu, X., & Song, F. (2023). Seasonal advance of intense tropical cyclones in a warming climate. *Nature*, 623(7985), 83–89. <https://doi.org/10.1038/s41586-023-06544-0>

Shi, J., Feng, X., Toumi, R., Zhang, C., Hodges, K. I., Tao, A., et al. (2024). Global increase in tropical cyclone ocean surface waves. *Nature Communications*, 15(1), 174. <https://doi.org/10.1038/s41467-023-43532-4>

Song, F., Leung, L. R., Lu, J., Dong, L., Zhou, W., Harrop, B., & Qian, Y. (2021). Emergence of seasonal delay of tropical rainfall during 1979–2019. *Nature Climate Change*, 11(7), 605–612. <https://doi.org/10.1038/s41558-021-01066-x>

Tang, Y., Huangfu, J., Huang, R., Chen, W., & Lan, X. (2024). Cluster analysis of the recent interdecadal variation in the tripole landfall pattern of tropical cyclones in East Asia. *Journal of Climate*, 37(18), 4885–4900. <https://doi.org/10.1175/JCLI-D-23-0413.1>

- Tu, J.-Y., Chou, C., & Chu, P.-S. (2009). The abrupt shift of typhoon activity in the vicinity of Taiwan and its association with western North Pacific–East Asian climate change. *Journal of Climate*, 22(13), 3617–3628. <https://doi.org/10.1175/2009JCLI2411.1>
- Van Rossum, G., & Drake, F. L. (2009). Python 3 reference manual [Software]. *CreateSpace*. Retrieved from <https://docs.python.org/3.9/>
- Walsh, K. J. E., McBride, J. L., Klotzbach, P. J., Balachandran, S., Camargo, S. J., Holland, G., et al. (2016). Tropical cyclones and climate change. *WIREs Climate Change*, 7(1), 65–89. <https://doi.org/10.1002/wcc.371>
- Wang, B., Yang, Y., Ding, Q.-H., Murakami, H., & Huang, F. (2010). Climate control of the global tropical storm days (1965–2008). *Geophysical Research Letters*, 37(7), L07704. <https://doi.org/10.1029/2010GL042487>
- Watanabe, M., & Jin, F.-F. (2003). A moist linear baroclinic model: Coupled dynamical–convective response to El Niño. *Journal of Climate*, 16(8), 1121–1139. [https://doi.org/10.1175/1520-0442\(2003\)16%3C1121:AMLBMC%3E2.0.CO;2](https://doi.org/10.1175/1520-0442(2003)16%3C1121:AMLBMC%3E2.0.CO;2)
- Wu, L., Wang, B., & Geng, S. (2005). Growing typhoon influence over East Asia. *Geophysical Research Letters*, 32, L18703. <https://doi.org/10.1029/2005GL022937>
- Ying, M., Zhang, W., Yu, H., Lu, X., Feng, J., Fan, Y., et al. (2014). An overview of the China Meteorological Administration tropical cyclone database [Dataset]. *Journal of Atmospheric and Oceanic Technology*, 31(2), 287–301. <https://doi.org/10.1175/JTECH-D-12-00119.1>
- Yokoi, S., Takayabu, Y. N., & Murakami, H. (2013). Attribution of projected future changes in tropical cyclone passage frequency over the western North Pacific. *Journal of Climate*, 26(12), 4096–4111. <https://doi.org/10.1175/JCLI-D-12-00218.1>
- Zhang, J., Wu, L., Ren, F., & Cui, X. (2013). Changes in tropical cyclone rainfall in China. *Journal of the Meteorological Society of Japan. Ser. II*, 91(5), 585–595. <https://doi.org/10.2151/jmsj.2013-502>
- Zhang, Q., Wu, L., & Liu, Q. (2009). Tropical cyclone damages in China 1983–2006. *Bulletin of the American Meteorological Society*, 90(4), 489–496. <https://doi.org/10.1175/2008BAMS2631.1>
- Zhao, J., Zhan, R., & Wang, Y. (2018). Global warming hiatus contributed to the increased occurrence of intense tropical cyclones in the coastal regions along East Asia. *Scientific Reports*, 8(1), 6023. <https://doi.org/10.1038/s41598-018-24402-2>
- Zhao, J., Zhan, R., Wang, Y., Xie, S.-P., & Wu, Q. (2020). Untangling impacts of global warming and Interdecadal Pacific Oscillation on long-term variability of North Pacific tropical cyclone track density. *Science Advances*, 6(41), eaba6813. <https://doi.org/10.1126/sciadv.aba6813>
- Zhao, J., Zhan, R., Wang, Y., & Xu, H. (2018). Contribution of the Interdecadal Pacific Oscillation to the recent abrupt decrease in tropical cyclone genesis frequency over the western North Pacific since 1998. *Journal of Climate*, 31(20), 8211–8224. <https://doi.org/10.1175/JCLI-D-18-0202.1>
- Zhou, X., Lu, R., & Chen, G. (2018). Impact of interannual variation of synoptic disturbances on the tracks and landfalls of tropical cyclones over the western North Pacific. *Advances in Atmospheric Sciences*, 35(12), 1469–1477. <https://doi.org/10.1007/s00376-018-8055-0>